Lattice Boltzmann model for simulating temperature-sensitive ferrofluids

Xiao-Dong Niu,* Hiroshi Yamaguchi, and Keisuke Yoshikawa
Department of Mechanical Engineering, Energy Conversion Research Center, Doshisha University, Kyoto 630-0321, Japan
(Received 29 September 2008; revised manuscript received 18 December 2008; published 28 April 2009)

In this paper, a lattice Boltzmann model for simulating temperature-sensitive ferrofluids is presented. The lattice Boltzmann equation for modeling the magnetic field is formulated using a scalar magnetic potential. Introducing a time derivative into the original elliptic equation for the scalar potential leads to an advection-diffusion equation, with an effective velocity determined by the temperature gradient. The time derivative is multiplied by an adjustable preconditioning parameter to ensure that the lattice Boltzmann solution remain close to a solution of the original elliptic equation for the scalar potential. To test the present lattice Boltzmann model, numerical simulations for the thermomagnetic nature convection of the ferrofluids in a cubic cavity are carried out. Good agreement between the obtained results and experimental data shows that the present lattice Boltzmann model is promising for studying temperature-sensitive ferrofluid flows.

DOI: 10.1103/PhysRevE.79.046713 PACS number(s): 47.11.−j, 47.65.Cb, 47.55.pb

I. INTRODUCTION

Ferrofluids are composed of magnetic nanoparticles suspended in a carrier fluid [1]. Such fine particles may be coated by a suitable surfactant to keep a stable suspension state and they can be treated as particles of single magnetic domain. The ferrofluids are a type of functional fluids whose flow and energy transport processes can be controlled by adjusting an external magnetic field. Due to this unique property, the ferrofluids have been applied to various aspects in practices such as heat pumps, energy conversion [2], and have also attracted a great deal of research interests from academics and industries [3,4].

Numerically, there are a number of different techniques for studying the ferrofluids [5,6], most of which are based on finite difference or finite volume methods, in which the continuum conservation equations and the Maxwell equations are discretized and solved on computational grids. An alternative approach, which is becoming increasingly popular, is the lattice Boltzmann (LB) method (LBM) [7]. The LBM has its solid root in kinetic theory and the general idea behind it is to compute a particle density distribution function, which represents fluid elements with a discrete velocity along the direction at spatial and temporal space as they move and collide on a lattice. The collective behavior of the distribution functions of the particles represents the dynamics of fluid flows. To date, several versions of the LBM have been used to study the magnetic fluid flows including magnetohydrodynamics (MHD) [8–11] or ferrohydrodynamics (FHD) [12–17] of the magnetic flows. However, directly solving the MHD or the FHD is difficult because the flux tensor of the electric field in the Maxwell equation is antisymmetric. The bidirectional streaming scheme of the tensor particle distribution function [8,10,12,13] and the vector-based distribution function technique [11,16,17] of the LBMs for simulating the MHD or the FHD have been proposed, respectively, to overcome the aforementioned difficulty and to model the magnetization evolution or the magnetic induction equation. These LBMs can model the magnetic field with the second-order time accuracy and in a wide range of magnetizations.

In this paper, a simpler LB model is presented to solve the Maxwell equation in simulating the temperature-sensitive ferrofluids. Different from the above LBMs [8,10–12,14,16,17], which consider the magnetoviscous effect due to noncollinear of the magnetization and magnetic intensity, the present LB model only concerns collinear situation in a narrow range of the magnetic-field strength and temperature. As a consequence of Coulomb's law, the Maxwell equation of the magnetic intensity can be written instead by an elliptic equation of the magnetic scalar potential [1,18]. Introducing a time derivative into the elliptic equation further leads to an advection-diffusion equation. By defining an effective velocity, which is a function of the temperature gradient, a LB scheme is straightforwardly constructed based on the advection-diffusion equation in a fashion of that for modeling the temperature transport equation. The present LB scheme has the first-order time accuracy. To ensure that the solution of the LB scheme remains close to a solution of the original elliptic equation for the scalar potential, the time derivative in the advection-diffusion equation is multiplied by an adjustable preconditioning parameter. This technique can also improve the convergence speed of solutions for steady-state flows. In contrast to the existing LBMs using tensor or vector-based distributions to model the magnetic field [8,10–13,16,17], the distribution function representing the magnetic field in the present scheme is a scalar, so variables and computer memory resources required by the present LB scheme are less than those of the existing models. Moreover, the numerical implementation of the present LB scheme for the magnetic field is straightforward and similar to that for the advection and diffusion of a scalar.

The rest of the paper is organized as follows. In Sec. II, we briefly give a description of the ferrofluid hydrodynamics. A short derivation of the magnetic force and the potential equation with a preconditioning parameter is presented. In Sec. III, a lattice Boltzmann scheme is introduced for the flow and magnetic field, respectively. Specifically, the lattice Boltzmann equation for the magnetic field is formulated in a similar form of the thermal lattice Boltzmann equation. Sec-

*Author to whom Correspondence should be address. xniu@mail.doshisha.ac.jp

 ©2009 The American Physical Society

tion IV focuses on the implementations of the boundary conditions and the numerical illustrations of the present LBM. The thermomagnetic nature convection of the ferrofluids in a cubic cavity is simulated. The results obtained are compared to the experimental measurements conducted in our laboratories. A conclusion is given in Sec. V.

II. FERROFLUID HYDRODYNAMICS

A. Governing equations

In the theory of the ferrofluids, a flow under an imposed magnetic field undergoes a magnetic force. The ferrofluid flow can be described by the following governing equations [1,18]

$$\partial_t \rho + \nabla \cdot (\rho \mathbf{u}) = 0, \tag{1}$$

$$\partial_t(\rho \mathbf{u}) + \nabla \cdot (\rho \mathbf{u}\mathbf{u}) = -\nabla\left(p + \mu_0 \int_0^H \left\{M - \rho\left(\frac{\partial M}{\partial \rho}\right)_{H,T}\right\} dH\right) + \eta\left[\nabla^2 \mathbf{u} + \frac{1}{3}\nabla(\nabla \cdot \mathbf{u})\right] + \mu_0 \mathbf{M} \cdot \nabla \mathbf{H} - \rho\beta(T - T_0)\mathbf{g}, \tag{2}$$

$$\left[\rho C_P - \mu_0 \mathbf{H} \cdot \left(\frac{\partial \mathbf{M}}{\partial T}\right)_H\right](\partial_t T + \mathbf{u} \cdot \nabla T) = \lambda \nabla^2 T - \left[\mu_0 T\left(\frac{\partial \mathbf{M}}{\partial T}\right)_H \cdot \frac{D\mathbf{H}}{Dt}\right], \tag{3}$$

$$\nabla \times \mathbf{H} = 0; \quad \nabla \cdot \mathbf{B} = 0. \tag{4}$$

In the above equations, $\mathbf{u}$ is the velocity field, D/Dt is the material derivative, $\nabla = \{\partial/\partial x, \partial/\partial y, \partial/\partial z\}$ with x, y, and z the axes of a three-dimensional system, ρ is the fluid density, p is the pressure, and T is the temperature. η is the dynamical viscosity and μ_0 is the magnetic permeability of vacuum, β is the expansion coefficient under the Boussinesq approximation. $\mathbf{H}$, $\mathbf{M}$, and $\mathbf{B}$ are the magnetic intensity, the magnetization, and the magnetic induction, respectively. λ is the thermal conductivity of the fluid, C_P is the specific heat at constant pressure.

B. Magnetic force

Given that magnetization is in equilibrium ($\mathbf{M}$ parallel to $\mathbf{H}$) and the magnetic induction is solenoid [$\nabla \cdot \mathbf{B} = 0$ and $\mathbf{B} = \mu_0(\mathbf{H} + \mathbf{M}) = \mu_0(1 + M/H)\mathbf{H} = \mu \mathbf{H}$], the magnetic force $\mu_0 \mathbf{M} \cdot \nabla \mathbf{H}$ can be simplified to

$$\mu_0 \mathbf{M} \cdot \nabla \mathbf{H} = \mu_0 \frac{M}{H} \mathbf{H} \cdot \nabla \mathbf{H} = \mu_0 \frac{M}{H}\left[\frac{1}{2}\nabla(\mathbf{H} \cdot \mathbf{H}) - \mathbf{H} \times (\nabla \times \mathbf{H})\right], = \mu_0 M \nabla H. \tag{5}$$

Equation (5) represents the component of the magnetic force per unit volume and depends on the existence of the magnetic gradient in the ferrofluids. Since for the normal flows, the magnetization depends only on the magnetic intensity $\mathbf{H}$ and the temperature T, the term $\mu_0 \int_0^H \{M - \rho(\partial M/\partial \rho)_{H,T}\} dH$ of Eq. (2) can thus be thus written by

$$\nabla \mu_0 \int_0^H \left\{M - \rho\left(\frac{\partial M}{\partial \rho}\right)_{H,T}\right\} dH = \mu_0 M \nabla H + \mu_0 \int_0^H \left(\frac{\partial M}{\partial T}\right)_H \nabla T dH + \frac{H^2}{2}\nabla \mu - \nabla\left[\rho\left(\frac{\partial \mu}{\partial \rho}\right)_T \frac{H^2}{2}\right]. \tag{6}$$

Generally, the magnetization of the magnetic fluid is a function of $\mathbf{H}$ and T. If the temperature field is nonuniform and the ferrofluid is thermosensitive, the magnetic force becomes the thermomagnetic driving force that may lead to thermomagnetic convection. In a narrow range of the magnetic intensity and the temperature, the magnetization M of the magnetic fluid can be given as [18]

$$M = \chi_0 H - K(T - T_0), \tag{7}$$

where $K = \chi_0 H/(T_c - T_0)$, T_0 and T_c are the reference and Curie temperatures, respectively, and χ_0 is magnetization rate at T_0. With Eq. (7) we have

$$\frac{M}{H} = \frac{\chi_0(T_s - T)}{T_s - T_0}, \tag{8}$$

$$\left(\frac{\partial M}{\partial T}\right)_H = -\chi_0 H/(T_c - T_0). \tag{9}$$

In most situations, the temperature range of an operated flow is far from the Curie temperature [$(\partial M/\partial T)_H = 0$]. Using Eqs. (5)–(9), and with the knowledge of the incompressible assumption [$\nabla \cdot \mathbf{u} = 0$ and $(\partial \mu/\partial \rho)_T = 0$], Eqs. (1)–(3) are reduced to the following equations:

$$\partial_t \rho + \nabla \cdot (\rho \mathbf{u}) = 0, \tag{10}$$

$$\partial_t(\rho \mathbf{u}) + \nabla \cdot (\rho \mathbf{u}\mathbf{u}) = -\nabla p + \eta \nabla^2 \mathbf{u} + \frac{\chi_0 \mu_0 H^2}{2(T_c - T_0)} \nabla T - \rho\beta(T - T_0)\mathbf{g}, \tag{11}$$

$$\partial_t T + \mathbf{u} \cdot \nabla T = \frac{\lambda(T_c - T_0)}{[\rho C_P(T_c - T_0) + \mu_0 \chi_0 H^2]} \nabla^2 T - \frac{\mu_0 \chi_0 H T \dfrac{DH}{Dt}}{[\rho C_P(T_c - T_0) + \mu_0 \chi_0 H^2]}. \tag{12}$$

C. Magnetic potential equation

For nonconductive flows, the magnetic intensity $\mathbf{H}$ and the magnetization $\mathbf{M}$ can be expressed as functions of a scalar potential ϕ as $\mathbf{H} = \nabla \phi$ [1,18]. Thus we can obtain an elliptic equation for ϕ from Eqs. (4) and (8) as

$$\partial_t \phi + \mathbf{u}_T \cdot \nabla \phi = \left[1 + \frac{\chi_0 (T - T_0)}{T_c - T_0} \right] \nabla^2 \phi, \tag{13}$$

where $\mathbf{u}_T = -\nabla(M/H) = \chi_0 \nabla T/(T_c - T_0)$ defines an effective velocity. The time derivative $\partial_t \phi$ is introduced in Eq. (13) to allow it to be solved in local time steps. To ensure that the LB solution of ϕ in Sec. III remains close to that of Eq. (13), an adjustable preconditioning parameter γ is multiplied $\partial_t \phi$ in Eq. (13) and we have

$$\frac{1}{\gamma} \partial_t \phi + \mathbf{u}_T \cdot \nabla \phi = \left[1 + \frac{\chi_0 (T - T_0)}{T_c - T_0} \right] \nabla^2 \phi. \tag{14}$$

III. LATTICE BOLTZMANN MODEL

A. Lattice Boltzmann schemes

In terms of the lattice Boltzmann theory [7,19], Eqs. (10)–(12) can be solved by the following lattice Boltzmann equations for the velocity and the temperature, respectively:

$$f_\alpha(\mathbf{r} + \boldsymbol{\xi}_\alpha \delta_t, t + \delta_t) - f_\alpha(\mathbf{r}, t) = -\frac{f_\alpha(\mathbf{r}, t) - f_\alpha^{eq}(\mathbf{r}, t)}{\tau_f} + w_\alpha \frac{(\tau_f - 0.5)\delta_t}{\tau_f c_s^2} \mathbf{F} \cdot (\boldsymbol{\xi}_\alpha - \mathbf{u}), \tag{15}$$

$$g_\alpha(\mathbf{r} + \boldsymbol{\xi}_\alpha \delta_t, t + \delta_t) - g_\alpha(\mathbf{r}, t) = -\frac{g_\alpha(\mathbf{r}, t) - g_\alpha^{eq}(\mathbf{r}, t)}{\tau_g} + w_\alpha S \delta_t, \tag{16}$$

with the respective equilibrium distribution functions given by

$$f_\alpha^{eq}(\mathbf{r}, t) = w_\alpha \rho \left\{ 1 + \frac{\boldsymbol{\xi}_\alpha \cdot \mathbf{u}}{c_s^2} + \frac{1}{2c_s^2} \left(\frac{(\boldsymbol{\xi}_\alpha \cdot \mathbf{u})^2}{c_s^2} - \mathbf{u}^2 \right) \right\}, \tag{17}$$

$$g_\alpha^{eq}(\mathbf{r}, t) = w_\alpha \frac{DT}{2} \left\{ \frac{\boldsymbol{\xi}_\alpha^2}{D c_s^2} + \frac{1}{D} \left(\frac{\boldsymbol{\xi}_\alpha^2}{c_s^2} - 2 \right) \frac{\boldsymbol{\xi}_\alpha \cdot \mathbf{u}}{c_s^2} + \frac{1}{2c_s^2} \left(\frac{(\boldsymbol{\xi}_\alpha \cdot \mathbf{u})^2}{c_s^2} - \mathbf{u}^2 \right) \right\}, \tag{18}$$

and the force $\mathbf{F}$ and the source S are written as

$$\mathbf{F} = \frac{\chi_0 \mu_0 H^2}{2(T_c - T_0)} \nabla T - \rho \beta (T - T_0) \mathbf{g}, \tag{19}$$

$$S = -\frac{\mu_0 \chi_0 H T \dfrac{DH}{Dt}}{[\rho C_P (T_c - T_0) + \mu_0 \chi_0 H^2]}, \tag{20}$$

where $\mathbf{r} = \mathbf{r}(x, y, z)$ is the spatial vector. The relaxation parameters in Eqs. (15) and (16) are determined by the viscosity and the thermal conductivity, respectively, as

$$\tau_f = \frac{\eta}{\rho_0 c_s^2 \delta_t} + 0.5, \tag{21}$$

$$\tau_g = \frac{D}{(D+2)} \frac{\lambda (T_c - T_0)}{[\rho C_P (T_c - T_0) + \mu_0 \chi_0 H^2)] c_s^2 \delta_t} + 0.5. \tag{22}$$

The sound speed c_s, the weight coefficient w_α, and the discrete velocity $\boldsymbol{\xi}_\alpha$ used in the above LBM scheme can be referred to the discrete velocity model of D2Q9 for two dimension (2D) and D3Q19 for three dimension (3D) [20]. The density, velocity, and temperature are calculated by

$$\rho = \sum_\alpha f_\alpha,$$

$$\rho \mathbf{u} = \sum_\alpha f_\alpha \boldsymbol{\xi}_\alpha + 0.5 \delta_t \mathbf{F},$$

$$T = \sum_\alpha g_\alpha. \tag{23}$$

For the thermal hydrodynamics, a number of previous researches [19,20] have shown by the Chapman-Enskog analysis, the lattice Boltzmann Eqs. (15) and (16) with Eqs. (17)–(23) be able to recover the macroscopic Eqs. (10) and (11) in the limit of low frequencies and long wavelengths, respectively.

B. Lattice Boltzmann equation for the magnetic potential

Equation (14) has a similar form of Eq. (12) and both are the advection/diffusion equations. Therefore, in a similar LBM fashion of Eq. (16) for the temperature, a lattice Boltzmann scheme for the magnetic potential can be constructed by introducing a microscopic magnetic potential distribution function h_α and it can be written as

$$h_\alpha(\mathbf{r} + \boldsymbol{\xi}_\alpha \delta_t, t + \delta_t) - h_\alpha(\mathbf{r}, t) = -\frac{h_\alpha(\mathbf{r}, t) - h_\alpha^{eq}(\mathbf{r}, t)}{\tau_h}. \tag{24}$$

The magnetic potential is calculated by an algebraic summation of the magnetic potential distribution function,

$$\phi = \sum_\alpha h_\alpha. \tag{25}$$

A crucial step in the developing a LBM is the selection of an appropriate single-particle equilibrium distribution function associated with vanishing of the collision operator. The magnetic potential equilibrium distribution function has to be consistent with definition of Eq. (25), and in addition has to give rise the correct magnetic dynamics. A suitable equilibrium distribution function fulfilling the above conditions can be given by

$$h_\alpha^{eq}(\mathbf{r}, t) = w_\alpha \phi \left\{ 1 + \frac{\boldsymbol{\xi}_\alpha \cdot \gamma \mathbf{u}_T}{c_s^2} + \frac{1}{2c_s^2} \left(\frac{(\boldsymbol{\xi}_\alpha \cdot \gamma \mathbf{u}_T)^2}{c_s^2} - (\gamma \mathbf{u}_T)^2 \right) \right\}. \tag{26}$$

By using the Chapmann-Enskog analysis, one can easily prove that Eq. (24) with Eqs. (25) and (26) recovers to the magnetic potential Eq. (14), and the relaxation parameter τ_h is determined through the following relation:

TABLE I. Cavity dimension, fluid properties used in present study.

Scale length of cavity L(mm)	5	Specific heat C_p (J/kg K)	1.387×10^5
Density ρ_0 (kg/m^3)	1397×10^3	Expansion coefficient β(1/K)	6.90×10^{-4}
Viscosity η (Pa s)	1.680×10^{-2}	Curie temperature T_c (K)	477.35
Thermal conductivity λ [W/(m K)]	1.570×10^{-1}	Reference temperature T_0(K)	298.15
Saturation magnetization M_s(A/m)	2.970×10^5	Magnetization rate χ_0	0.2650
Permeability of vacuum μ_0(H/m)	$4\pi\times10^{-7}$	Gravitational acceleration g(m/s^2)	9.8

$$\tau_h = \frac{\gamma}{c_s^2\delta_t}\left[1+\frac{\chi_0(T-T_0)}{T_c-T_0}\right]+0.5. \tag{27}$$

The flow field and the magnetic field are coupled for the temperature-sensitive magnetic fluid flows, and Eqs. (19), (20), (22), and (27) clearly show this mechanism mesoscopically. In numerical implementation, the preconditioned parameter can be given by letting the value of τ_h around 1.

IV. NUMERICAL SIMULATIONS

To test the present lattice Boltzmann model, numerical simulations for the thermomagnetic nature convection of the ferrofluids in a cubic cavity under uniform magnetic field are carried out. The case chosen in this simulation are in line with our experimental conditions [21], which are given in Table I. The cavity (Fig. 1) sealed with rigid walls is filled with a thermal sensitive magnetic fluid, and it is heated and cooled from the bottom and upper walls, respectively. The side walls of the cavity are insulated. In the numerical simulations, a uniform magnetic intensity H_0 is imposed along the opposite direction of the gravitation. The value of H_0 and the temperature difference $\Delta T=T_b-T_u$ between the upper and bottom walls are given by the Rayleigh number Ra $=\rho_0 g\beta\Delta TL^3/(k\eta)$ and the magnetic Rayleigh number Ram $=\mu_0 H_0 M_s L^2/(k\eta)$, where $k=\lambda/\rho_0 C_P$ is the thermal diffusivity. The boundary conditions can be referred in Fig. 1. For the magnetic field, the magnetic potential boundary conditions are set by the magnetic intensity, which are described as follows:

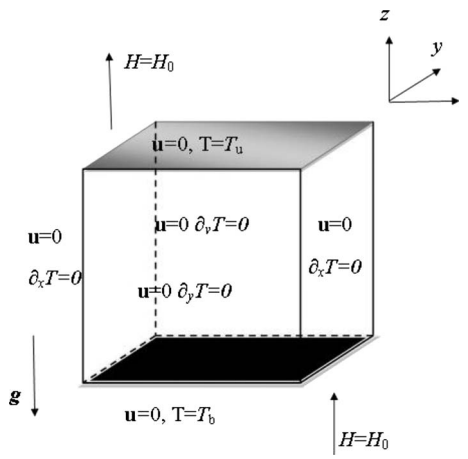

FIG. 1. Sketch of the thermomagnetic nature convection flow conditions in the cubic cavity.

$$\left.\frac{\partial\phi}{\partial x}\right|_{x=0,L}=0,\qquad \left.\frac{\partial\phi}{\partial y}\right|_{y=0,L}=0,\qquad \left.\frac{\partial\phi}{\partial z}\right|_{z=0,L}=\frac{H_0}{(1+\chi)}, \tag{28}$$

where $\chi=\chi_0(T_c-T)/(T_c-T_0)$.

For the distribution functions of f_α and g_α on the boundaries, the nonequilibrium bounce back boundary conditions [19] are employed when the macroscopic velocity and temperature on the solid walls are calculated. Here, we just briefly give the formulation and detailed can be referred to Ref. [19]. The nonequilibrium bounce back boundary conditions for velocity and temperature are

$$f_{\bar\alpha}(\mathbf{r},t)-f^{eq}_{\bar\alpha}(\mathbf{r},t)=f_\alpha(\mathbf{r},t)-f^{eq}_\alpha(\mathbf{r},t), \tag{29}$$

$$g_{\bar\alpha}(\mathbf{r},t)-g^{eq}_{\bar\alpha}(\mathbf{r},t)-\xi^2_{\bar\alpha}[f_{\bar\alpha}(\mathbf{r},t)-f^{eq}_{\bar\alpha}(\mathbf{r},t)] = -\{g_\alpha(\mathbf{r},t)-g^{eq}_\alpha(\mathbf{r},t)-\xi^2_{\bar\alpha}[f_\alpha(\mathbf{r},t)-f^{eq}_\alpha(\mathbf{r},t)]\}, \tag{30}$$

where $\bar\alpha$ denotes directions of the unknown distribution function, and $\bar\alpha=-\alpha$. For the magnetic potential field, a similar fashion of Eq. (29) is formulated in this paper. This scheme enabled the magnetic potential to be specified at the boundaries, which is generally equivalent to impose a constant magnetic intensity on the boundaries. Specifically, the unknown potential distribution function $h_{\bar\alpha}(\mathbf{r},t)$ is calculated as

$$h_{\bar\alpha}(\mathbf{r},t)-h^{eq}_{\bar\alpha}(\mathbf{r},t)=-[h_\alpha(\mathbf{r},t)-h^{eq}_\alpha(\mathbf{r},t)]. \tag{31}$$

Table II presents a comparison of the calculated average Nusselt numbers [Nu$=\iint(-\partial T/\partial Z)_{z=0,L}dxdy$] of the natural convection flows under pure gravitation over a range of Rayleigh numbers from 4000 to 10000 obtained for different

TABLE II. A comparison of the calculated average Nusselt numbers of natural convection flows under pure gravity force over a range of Rayleigh numbers from 4000 to 10000 obtained for different grids.

	Nu		
Ra	$31\times31\times31$	$41\times41\times41$	$51\times51\times51$
4000	1.2045	1.1961	1.1933
5000	1.4341	1.4203	1.4167
6000	1.5738	1.5540	1.5501
8000	1.7193	1.7012	1.6992
10000	1.8255	1.8146	1.8097

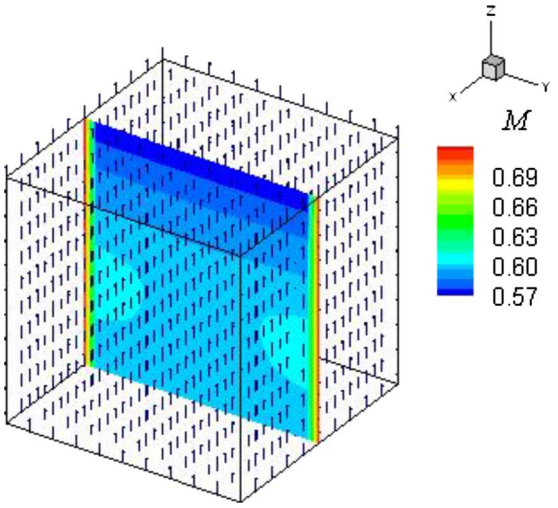

FIG. 2. (Color online) The calculated magnetic intensity field and the contours of modulus of the magnetization in y-z plane of $x=0.5$ in the cubic cavity for Ra=5000 and Ram=1.00×10^8.

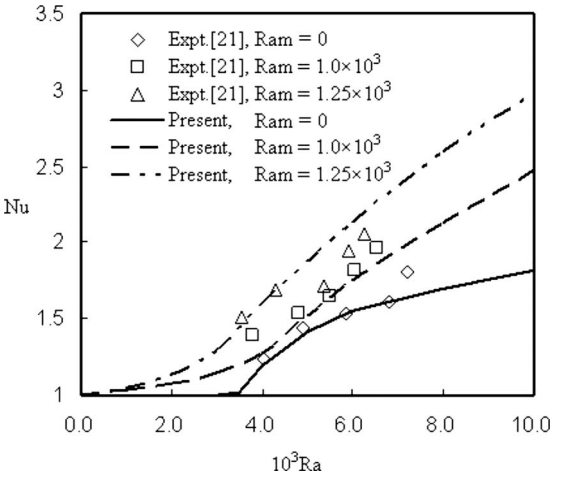

FIG. 3. Dependence of the average Nusselt numbers on the Rayleigh numbers at three magnetic Rayleigh numbers of 0, 1.00×10^8, and 1.25×10^8. (a) Ram=1.00×10^8 and (b) Ram=1.25×10^8.

grids, it is clear that the moderate grids of $41\times41\times41$ describes the behavior of the system fairly well. Thus, all the following results presented will be based on the $41\times41\times41$ grid unless otherwise mentioned.

Figure 2 shows that the calculated magnetic intensity field in the cubic cavity at Ra=5000 and Ram=1.00×10^8. The magnetic intensity **H** can be evaluated from definition of $\mathbf{H}=\nabla\phi$ by using the second-order central finite differencing. It should be addressed that all the gradients appeared in the above Eqs. (15)–(26) are calculated by using the second-order central differencing. As the magnetization **M** is everywhere parallel to the magnetic field **H** in the flow field, the contours of modulus of the magnetization are plotted in y-z plane of $x=0.5$ in the cubic cavity. The modulus of **M** is calculated directly by Eq. (8). As shown in Fig. 2, the magnetic intensity vectors parallel each other and are aligned with the positive z coordinate. Due to nature convection effects and the temperature dependence of the magnetization, the modulus of the magnetization **M** is shown to be varied in the cavity. Large magnetization is found near the side isolated walls and low magnetization appeared in central region.

The nature convection flows in a cubic cavity is usually considered as a standard benchmark case. Earlier studies [22,23] showed that the convection roll only occurs above a critical Rayleigh number $Ra_c\approx3350$ under the pure gravitational force. When magnetic field is imposed, it is expected the heat transfer is enhanced inside cavity. Figure 3 displays the dependence of the average Nusselt numbers on the Rayleigh numbers at three magnetic Rayleigh numbers of 0, 1.00×10^8, and 1.25×10^8. For comparison, experimental data [21] are also included in this figure. Seen from Fig. 3, with the increase in the imposed magnetic intensity, the Nusselt numbers are increased accordingly, which denotes the enhancement of the heat transfer inside the cavity. For Ram=0, no imposed magnetic field, it is found that the nature convection occurs above a critical Rayleigh number of $Ra_c\approx3400$. This observation is agreed with the earlier studies [22,23]. Moreover, compared to the experiment data [21],

Fig. 3 shows that the present model gives a good prediction of the thermomagnetic nature convection ferrofluid flows in the cubic cavity. Figures 4(a) and 4(b) show the midplane flow patterns and temperature fields of Ra=5000 inside the cavity at Ram=1.00×10^8 and 1.25×10^8, respectively. As shown in Figs. 4(a) and 4(b), between the heated bottom wall and the cooled upper wall, a weak flow roll occurs under the magnetic forces. The main flows bring the low-temperature fluid downward, and the high-temperature fluid is brought

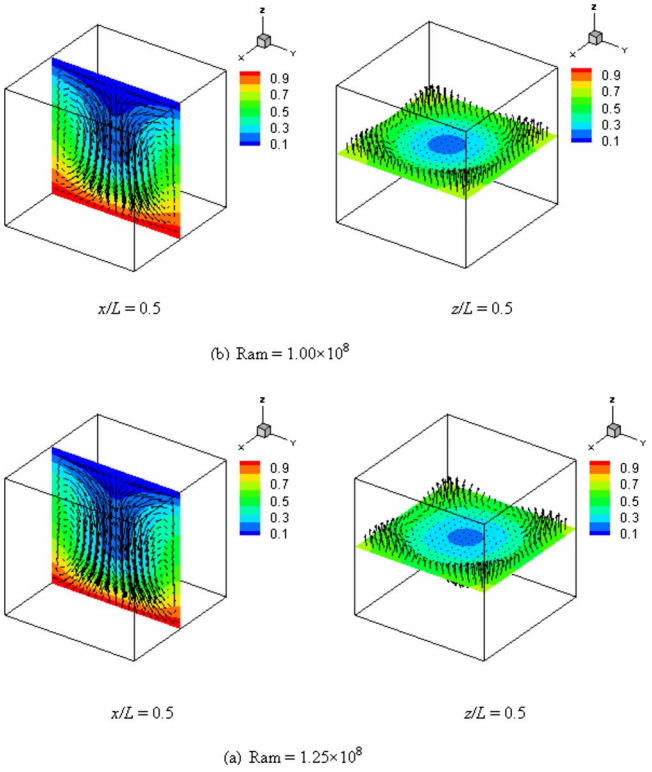

FIG. 4. (Color online) The midplane flow patterns and temperature fields of Ra=5000 inside the cavity at Ram=1.00×10^8 and 1.25×10^8, respectively.

upward from regions near the sidewalls. The larger the magnetic Rayleigh number, the faster the heated transportation in the cavity.

V. CONCLUSIONS

In this paper, a LB model for the temperature-sensitive ferrofluids is presented. The LB scheme for simulating the magnetic field is formulated based on the advection-diffusion equation of the scalar magnetic potential. An effective velocity related to the temperature gradient is defined. To ensure that the LBM solution remains close to a solution of the original elliptic equation for the magnetic potential, an adjustable preconditioning parameter is multiplied to the time derivative in the advection/diffusion equation. To test the present lattice Boltzmann model, numerical simulations for the thermomagnetic nature convection of the ferrofluids in a cubic cavity under uniform magnetic field are carried out. Good agreement between the obtained results and the experimental data shows that the present lattice Boltzmann model is promising for studying temperature-sensitive ferrofluid flows.

ACKNOWLEDGMENTS

This work was supported by a grant-in-aid for Scientific Research (C) from the Ministry of Education, Culture, Sports, Science, and Technology, Japan.

[1] R. E. Rosensweig, *Ferrohydrodynamics* (Cambridge University Press, London, 1985).
[2] R. Hiergeist, W. Andra, N. Buske, R. Hergt, I. Hilger, U. Richter, and W. Kaiser, J. Magn. Magn. Mater. **201**, 420 (1999).
[3] S. Shuchi, K. Sakatani, and H. Yamaguchi, J. Magn. Magn. Mater. **289**, 257 (2005).
[4] A. Hatch, A. E. Kamholz, G. Holman, P. Yager, and K. F. Böhringer, J. Microelectromech. Syst. **10**, 215 (2001).
[5] S. M. Snyder, T. Cader, and B. A. Finlayson, J. Magn. Magn. Mater. **262**, 269 (2003).
[6] J. Mizushima and T. Nakamura, J. Phys. Soc. Jpn. **72**, 197 (2003).
[7] S. Chen and G. D. Doolen, Annu. Rev. Fluid Mech. **30**, 329 (1998).
[8] S. Chen, H. Chen, D. O. Martinez, and W. H. Matthaeus, Phys. Rev. Lett. **67**, 3776 (1991).
[9] S. Succi, M. Vergassola, and R. Benzi, Phys. Rev. A **43**, 4521 (1991).
[10] D. O. Martinez, S. Chen, and W. H. Matthaeus, Phys. Plasmas **1**, 1850 (1994).
[11] P. J. Dellar, J. Comput. Phys. **179**, 95 (2002).
[12] M. Hirabayashi, Y. Chen, and H. Ohashi, Phys. Rev. Lett. **87**, 178301 (2001).
[13] M. Hirabayashi, Y. Chen, and H. Ohashi, Comput. Phys. Commun. **142**, 148 (2001).
[14] V. Sofonea and W. G. Frueh, Eur. Phys. J. B **20**, 141 (2001).
[15] Y. Xuan, M. Ye, and Q. Li, Int. J. Heat Mass Transfer **48**, 2443 (2005).
[16] J. Walley, MS thesis, University of Oxford, 2003.
[17] P. J. Dellar, J. Stat. Phys. **121**, 105 (2005).
[18] H. Yamaguchi, *Engineering Fluid Mechanics* (Springer, Netherlands, 2008).
[19] X. He, S. Chen, and G. D. Doolen, J. Comput. Phys. **146**, 282 (1998).
[20] D. A. Wolf-Gladrow, *Lattice-Gas Cellular Automata and Lattice Boltzmann Models* (Springer-Verlag, Berlin, 2000).
[21] T. Kato, MS thesis, Doshisha University, 2007.
[22] W. L. Heitz and J. W. Westwater, ASME Trans. J. Heat Transfer **C93**, 188 (1971).
[23] I. Catton, Int. J. Heat Mass Transfer **15**, 665 (1972).